Node generation in complex 3D domains for heat conduction problems solved by RBF-FD meshless method

To cite this article: Riccardo Zamolo and Enrico Nobile 2021 *J. Phys.: Conf. Ser.* **2116** 012020

View the article online for updates and enhancements.

Node generation in complex 3D domains for heat conduction problems solved by RBF-FD meshless method

Riccardo Zamolo and Enrico Nobile

Dipartimento di Ingegneria e Architettura, Università degli Studi di Trieste, via A. Valerio 10, 34127 Trieste, Italy

E-mail: `rzamolo@units.it`

Abstract. A novel algorithm is presented and employed for the fast generation of meshless node distributions over arbitrary 3D domains defined by using the stereolithography (STL) file format. The algorithm is based on the node-repel approach where nodes move according to the mutual repulsion of the neighboring nodes. The iterative node-repel approach is coupled with an octree-based technique for the efficient projection of the nodes on the external surface in order to constrain the node distribution inside the domain. Several tests are carried out on three different mechanical components of practical engineering interest and characterized by complexity of their geometry. The generated node distributions are then employed to solve a steady-state heat conduction test problem by using the Radial Basis Function-generated Finite Differences (RBF-FD) meshless method. Excellent results are obtained in terms of both quality of the generated node distributions and accuracy of the numerical solutions.

1. Introduction

When solving engineering problems over complex geometries using mesh-based methods, grid generation can be really burdensome and represents a very crucial phase in the whole simulation process. Meshless methods [1] therefore possess great potential advantages over mesh-based methods, since no mesh is needed. The problem of mesh generation is then turned into a node generation problem, which is theoretically easier.

Fast and simple node generation algorithms have already been developed in 2D [2, 3] and 3D [4] cases. Nonetheless, to the best of authors' knowledge, there is no efficient and robust 3D node generator which is fully node-based and specifically designed to face arbitrary and complex geometries required in practical engineering problems. In this paper we present an efficient approach which fulfill these requirements, being able to generate 3D node distributions over arbitrary geometries defined by using the stereolithography (STL) file format. Three STL models, namely a pin, a crankcase and a screw (see Figure 1), will be employed.

In order to assess the suitability and the validity of the generated node distributions for meshless discretizations, these distributions will be employed to solve a steady-state heat conduction problem by using the Radial Basis Function-generated Finite Differences (RBF-FD) meshless method [5–7]. The accuracy of the numerical solutions will be assessed by performing convergence tests for each of the three models.
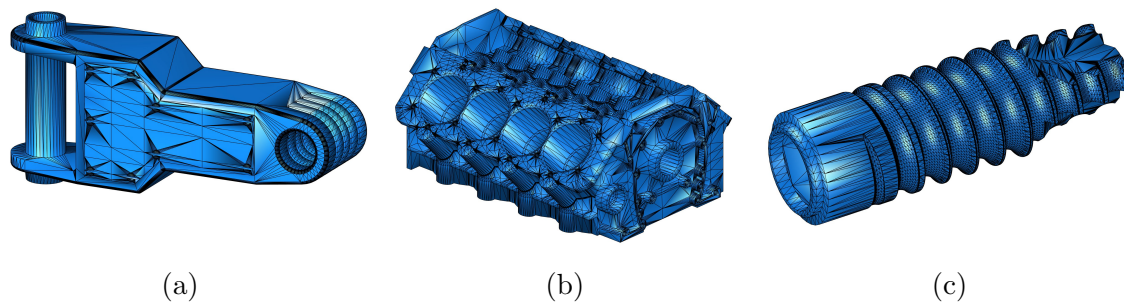
Figure 1. STL models of three mechanical components: pin (a), 9216 triangles; crankcase (b), 41414 triangles; screw (c), 68992 triangles.

Table 1. Number of octree boxes generated by the algorithm with minimum box size h_m and maximum number of triangles $T_M = 10$.

$-\log_8(h_m)$	1	2	3	4	5	6	7	8
Pin	169	8233	62089	71745	72225	72225	72225	72225
Crankcase	329	40353	261569	292145	295537	295929	295929	295929
Screw	185	16721	269721	508809	536793	542721	543249	543249

2. Methodology

2.1. Octree space partitioning

In a STL model, a 3D object is described by an unstructured triangulated surface. Therefore, in order to efficiently compute any geometrical operation, e.g., minimum distance from a node to the surface, projection of a node onto the surface, inside/outside test, etc., a triangle-based octree partitioning [8] of the space around the object is performed. The recursive subdivision of the space into octants is carried out by fulfilling the following rules:

- each leaf-box, i.e., box with no children, can not contain more than T_M triangles
- the minimum size of each leaf-box is h_m
- the first constraint can be ignored if a box and its parent-box both contain exactly one vertex of the triangulated surface, which is also the same vertex

where the last rule avoids infinite octree subdivisions around nodes connected to more than T_M triangles. The effectiveness of the last rule is confirmed by the results reported in Table 1, where the total number of octree boxes reaches a maximum and does not grow indefinitely when the minimum box size h_m is reduced. A graphical representation of the octree space partitioning is depicted in Figure 4.

2.2. Initial node positioning and node-repel approach

Given a prescribed spacing function s, which is chosen to be constant for the sake of simplicity, an octree-based algorithm modified with a dithering correction is employed to generate an initial node distribution [9]. The node distribution is then refined by means of an iterative node-repel approach [2, 3, 9] using 36 neighboring nodes. In this phase the octree data structure is employed to efficiently project onto the surface the nodes leaving the domain.
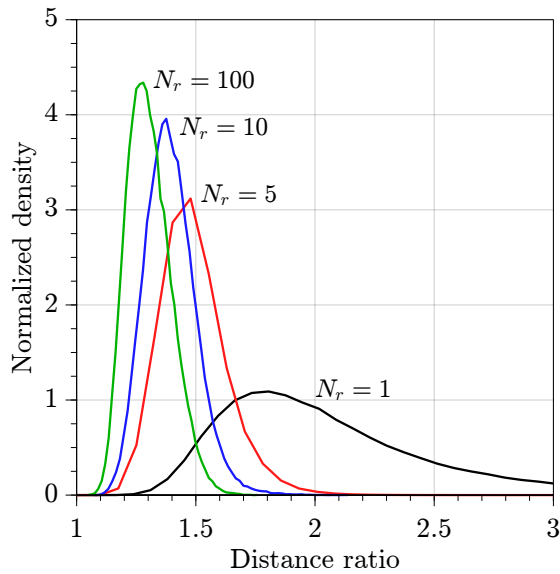
Figure 2. Normalized distribution of distance ratio after N_r repel iterations, crankcase model with 200,000 nodes.
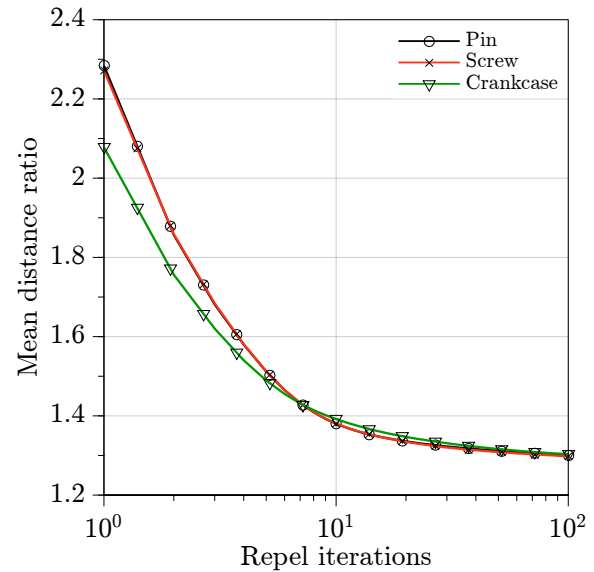
Figure 3. Convergence history of mean distance ratio with 200,000 nodes for each model.

2.3. RBF-FD method

The RBF-FD meshless method [5, 6] is employed to discretize the following 3D Poisson equation in the unknown temperature field T:

$$-\nabla^2 T = b \tag{1}$$

with Dirichlet boundary conditions. The multiquadric basis function has been employed, where the chosen shape factor is $\varepsilon = 0.2/s$ [10].

3. Results

3.1. Node generation

Figure 2 shows the normalized distribution of the distance ratio after N_r repel iterations. The distance ratio is the ratio of maximum to minimum distances between the 12 nearest nodes and can be interpreted as an isotropic quality index of the local node arrangement with respect to face-centered cubic or hehagonal close-packed 3D lattices. The effect of repel iterations is to tighten and shift the distribution towards smaller values of the distance ratio, as expected. This is also confirmed by the convergence curves of the mean distance ratio for the whole node distribution, reported in Figure 3, where a rapid decrease is then followed by an asymptotic behaviour. An example of node distribution for the crankcase model is depicted in Figure 5 and 6, where the high quality of the boundary distribution can be appreciated.

3.2. RBF-FD

Convergence tests are carried out for polynomial order $P = 2, 3$ and $n = 30, 60$ supporting nodes, respectively [11]. The chosen analytical solution is:

$$T = \sin(2\pi x)\sin(2\pi y)\sin(2\pi z) \tag{2}$$

and each model has been scaled in order to fit into the unit cube $[0, 1]^3$. A graphical representation of the temperature field T over the crankcase model is depicted in Figure 7.
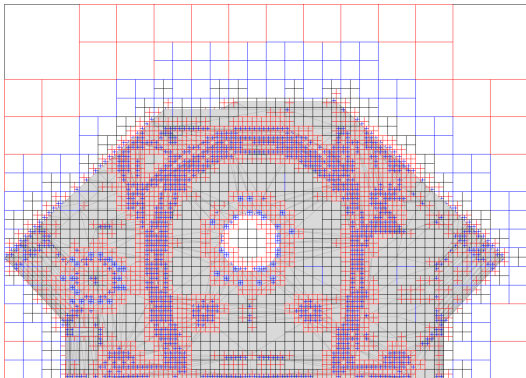
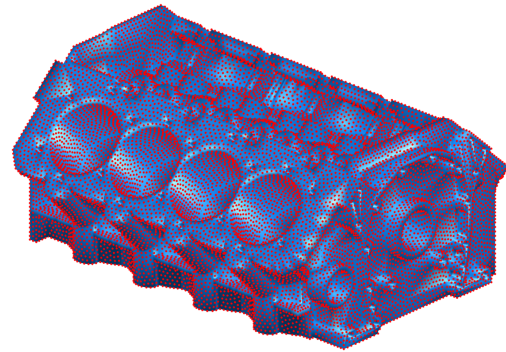**Figure 4.** Side view of the generated octree for the crankcase model, $h_m = 1/256$ and $T_M = 5$.

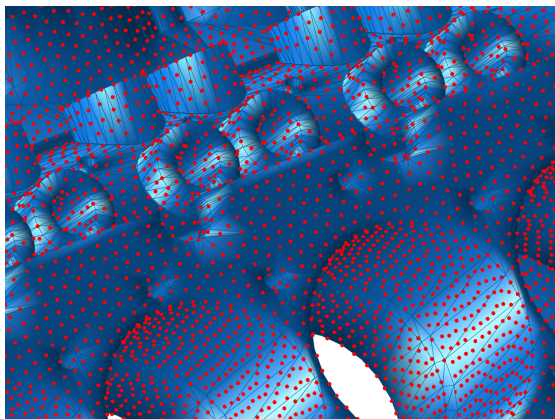**Figure 5.** Node distribution with 100,000 nodes after 100 repel iterations.

Figure 6. Enlarged view of a particular of the node distribution over the crankcase model with 100,000 nodes.
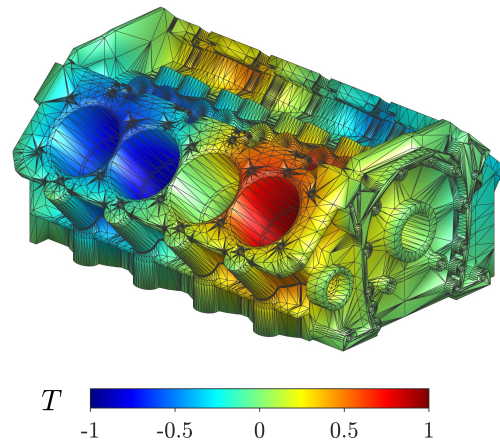

Figure 7. Computed temperature field over the crankcase model for the problem of Eq. (1).

The convergence curves are depicted in Figure 8, highlighting an order of accuracy varying from $p = 2.1$ to $p = 2.9$. Unexpectedly, the highest order of accuracy, i.e., $p = 2.9$, is obtained in the case $P = 2$, while p is lower and close to 2.0 in the case $P = 3$. This is probably due to the fact that in the latter case the supporting radius, i.e., $n = 60$ neighboring nodes, is too large to fit correctly into some of the small details and narrow walls of the complex geometries employed. It's conceivable that the use of a variable spacing function to account for the complex geometry can positively affect this unexpected behaviour.

4. Conclusions
In this paper a novel node generation algorithm has been proposed. This algorithm, based on a node-repel approach, is capable of generating high quality 3D node distributions over arbitrary geometries described by STL files. These distributions are suitable for the use with meshless
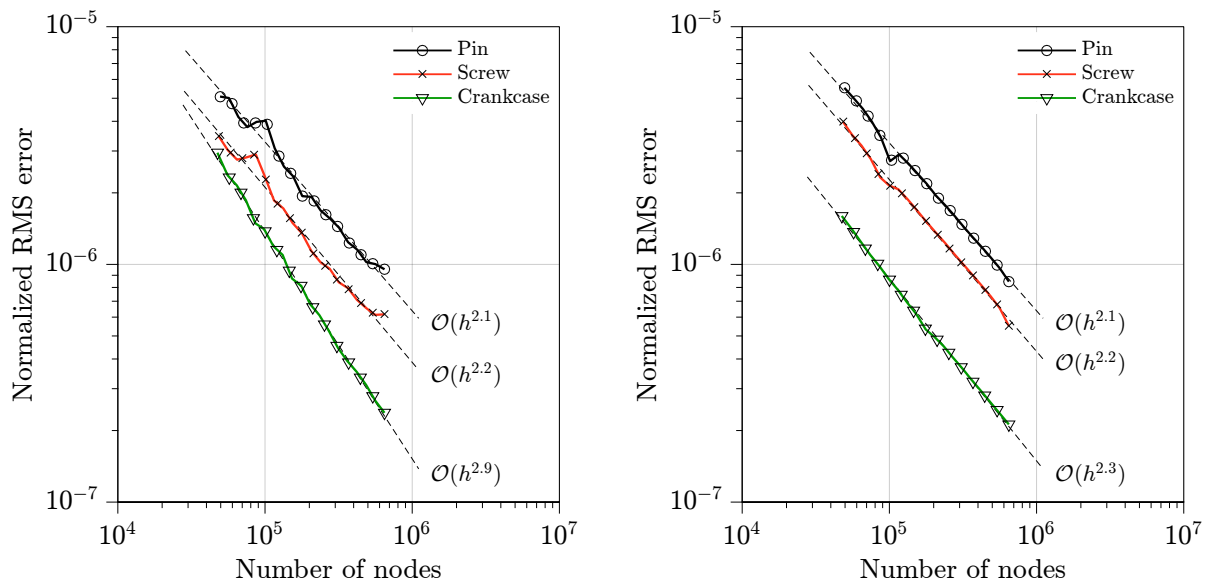
Figure 8. Normalized root mean square error for polynomial order $P = 2$ and $n = 30$ support nodes (left), $P = 3$ and $n = 60$ (right).

methods, in particular with the RBF-FD method for which good convergence properties have been obtained with three complex 3D models of mechanical components of practical engineering interest in the case of a steady-state heat conduction problem.

References
[1] Li H and Mulay S 2013 *Meshless Methods and Their Numerical Properties* (CRC Press) ISBN 978-1-4665-1747-9
[2] Fornberg B and Flyer N 2015 *Comput. Math. Appl.* **69** 531–544
[3] Zamolo R and Nobile E 2018 *Comput. Math. Appl.* **75** 4305–4321
[4] Vlasiuk O, Michaels T, Flyer N and Fornberg B 2018 *Comput. Math. Appl.* **76** 1739–1757
[5] Šarler B and Vertnik R 2006 *Comput. Math. Appl.* **51**(8) 1269–1282
[6] Fornberg B and Flyer N 2015 *Acta Numer.* **24** 215–258
[7] Zamolo R, Nobile E and Šarler B 2019 *J. Comput. Phys.* **392** 311–334
[8] de Berg M, Cheong O, van Kreveld M and Overmars M 2008 *Computational Geometry* (Springer-Verlag Berlin Heidelberg) ISBN 978-3-540-77974-2
[9] Zamolo R 2019 *Radial Basis Function-Finite Difference Meshless Methods for CFD Problems* Ph.D. thesis Università degli Studi di Trieste Trieste, Italy
[10] Sarra S and Kansa E 2009 *Multiquadric Radial Basis Function Approximation Methods for the Numerical Solution of Partial Differential Equations* (*Advances in Computational Mechanics* vol 2) (Tech Science Press)
[11] Bayona V, Flyer N, Fornberg B and Barnett G 2017 *J. Comput. Phys.* **332** 257–273